

# Learning Movement Assessment Primitives for Force Interaction Skills

Xiang Zhang, Athanasios S. Polydoros and Justus Piater

**Abstract**—We present a novel, reusable and task-agnostic primitive for assessing the outcome of a force-interaction robotic skill, useful e.g. for applications such as quality control in industrial manufacturing. The proposed method is easily programmed by kinesthetic teaching, and the desired adaptability and reusability are achieved by machine learning models. The primitive records sensory data during both demonstrations and reproductions of a movement. Recordings include the end-effector’s Cartesian pose and exerted wrench at each time step. The collected data are then used to train Gaussian Processes which create models of the wrench as a function of the robot’s pose. The similarity between the wrench models of the demonstration and the movement’s reproduction is derived by measuring their Hellinger distance. This comparison creates features that are fed as inputs to a Naive Bayes classifier which estimates the movement’s probability of success. The evaluation is performed on two diverse robotic assembly tasks – snap-fitting and screwing – with a total of 5 use cases, 11 demonstrations, and more than 200 movement executions. The performance metrics prove the proposed method’s capability of generalization to different demonstrations and movements.

## I. INTRODUCTION

Despite the large research interest on generic motion representation models in robotics (e.g. motion primitives)[1], the development of corresponding methods for assessing the robot-environment interaction is rather poor. The significance of such models rises by the need of robotic manufacturing processes to rapidly evaluate the effect of motions. Especially, mass customized production demands smart, adaptable and collaborative robotic systems instead of hard-coded caged robots. Therefore, such robotic systems have to self-evaluate their performance via methods which can adapt to a large variety of tasks by minimum reprogramming. Those needs can be met by developing robots equipped with abstract and easily adaptable functionalities: the primitives.

Primitives are commonly trained by imitation learning or Programming by Demonstration (PbD) [2] methods which facilitates fast re-programming by non-experts. In collaborative robots, a trajectory can be assigned much more intuitively by kinesthetic teaching [3] compared to hard-coded programming. The data collected during kinesthetic teaching are used to adapt the primitives on the desired task via supervised or reinforcement learning [4]. Thus, kinesthetic teaching, in conjunction with machine learning

All the authors are with Intelligent & Interactive Systems (IIS), Department of Computer Science, Universität Innsbruck, 6020 Innsbruck, Austria {firstname.lastname}@uibk.ac.at

The research leading to these results is funded by the Austrian Federal Ministry of Transport, Innovation and Technology (BMVIT) under the program “ICT of the Future” and project number 855425, FlexRoP.

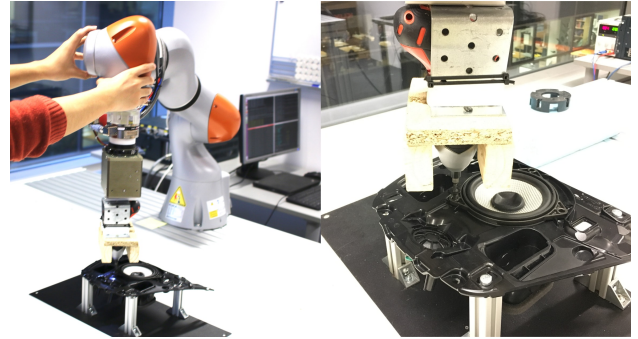


Fig. 1: A KUKA iiwa equipped with an ATI F/T sensor learns how to perform a task from human demonstrations (left), and reproduce the task in novel situation (right). Motion Assessment Primitives (MAPs) are employed for assessing the movement’s reproduction performance.

approaches, provides an appealing method for non-experts to program a robotic system.

Nevertheless, solely the motion primitives are not sufficient to guarantee successful task executions since uncertainties from the environment may cause failures. Therefore, an additional model is required to assess the outcome which can enable the robotic system to detect its failures and even self-improve its skills via reinforcement learning. Thus, a skill-based learning system should include both assessment and motion primitives in order to increase its adaptability and performance.

Therefore, this paper introduces the concept of Movement Assessment Primitives (MAPs). Similar to dynamic movement primitives (DMPs), MAPs are abstract elementary blocks which are automatically adapted on various tasks via machine learning in order to evaluate the motions of robotic manipulators. Furthermore, they are generic enough to be applied on a wide variety of tasks without the need of reprogramming. Thus, they significantly differ from traditional methods of motion assessment in skill-based systems which require knowledge about the performed task [5].

In this paper, MAPs are kinesthetically taught from demonstrations and capture the pose and applied wrench on the end-effector during the robot’s movement. The aforementioned data are used to create wrench models which represent the expected wrench at each pose of the manipulator. The wrench models, which derive from the expert demonstration, are compared with those created from a movement reproduction. Their similarity measurement is treated as a feature of a binary probabilistic classifier which assigns a probability

of success for each reproduced movement. The proposed method is evaluated on five use-cases of robotic assembly operations, namely, on three mechanisms of snap-fitting and two screwing.

Thus, the main *contribution* of this paper is a novel task-agnostic machine learning approach for automatic assessment of force-interaction skills. The proposed method focuses on the effect of the robot-environment interaction, which is the observed wrench, rather than the cause, *i.e.* the trajectory itself. Furthermore, there is no assumption regarding the performed task and hence it can be part of any force-interaction skill. Moreover, it is able to generalize on a variety of movements with different demonstrations, initial and target states.

## II. RELATED WORK

The assessment of a task execution requires modeling of sensory data. Such data-driven approaches are followed for fault-detection at process monitoring applications. In this field, the system is modeled by Ordinary Differential Equation (ODE) [6]. However, in PbD, velocity and acceleration vary for different human demonstrations and also a human is able to apply arbitrary force, but the force applied by a robot is limited by constraints such as motors, safe and impedance settings [7] etc. Therefore, the robot cannot identically reproduce the force demonstrated by a human which makes the modeling of demonstrations via ODE rather challenging.

An alternative solution to assess the task outcome is statistically setting a threshold regarding the wrench signature and the pose trajectories. Costa *et al.*[8] verify the success of a process by setting a threshold for eccentricity and typicality, *i.e.* distance metrics for time series. Haidu *et al.*[9] define lower and upper bounds of the trajectory profile based on successful trails. Thus, trajectory profiles that exceed the threshold indicates a failure. Nevertheless, the movement reproduction varies for different task parameters (e.g. start and goal state) and demonstrations. In those cases, the bounds have to be changed accordingly which requires reprogramming.

Rojas *et al.*[10] identify key segments of the wrench signals and create a task-specific hierarchical taxonomy based on its time derivative. The task outcome is indicated by the states at the highest level of this taxonomy. However, the segmentation threshold is predefined, and the taxonomy associated with segments is manually created which significantly reduces its applicability to different tasks.

Haidu *et al.*[11] segment the task in smaller pose trajectories and train a Hidden Markov Model (HMM) using each segment as a state. They identify promising states by aligning the segmented samples to the HMM, which contains key information for failure detection. A predictor is trained to assess the task from the aligned data at those promising states. Similarly, Di Lello *et al.*[12] segment the wrench signatures by the control strategy of a finite state machine. Each wrench signal is treated as a Bayesian time-series model. A HMM is trained via a Bayesian non-parametric method to

detect the deviation from the successful execution. Both of those two methods require the predefined segmentation of the trajectory. However, there is often no such clear segmentation such as Zero Velocity Crossing point [13] or contact events that are plausible in human demonstrations.

In the field of imitation learning, Calinon *et al.*[14] evaluate a movement in order to optimize a controller. Firstly they align the recorded demonstrations with Hidden Markov Model (HMM) and project them into a latent space via PCA. Then they measure the weights of each vector in the latent space by the variations in multiple demonstrations subject to the same task constraint. Eventually, a similarity measure is defined by the weighted sum of Euclidean distances between a new trajectory and the successful one. The application of this method does not involve wrench in the task and also requires a preprocessing procedure which increases the complexity of implementation.

In the field of reinforcement learning, Pastor *et al.*[15] propose an algorithm which learns the outcome of an assessment system given a predefined threshold based on a reward function. The system is merged with reinforcement learning framework. However, the definition of the reward function may be challenging for certain tasks and also limits the method's re-usability.

The aforementioned methods assess the task outcome with regard to wrench signatures or pose profiles separately. Thus, they do not take into account any dependence between wrench and state which characterizes a force-interaction task. Contrary, the proposed method takes into account this dependency by creating a wrench model which maps state to wrenches. Furthermore, the relative state w.r.t the motion's goal state is used as input to the proposed model. In such way is achieved the desired generalization of the method to different starting and goal states. Moreover, a similarity score between the wrench models of the movement demonstration and reproductions is used in order to assess the movement. This facilitates generalization across multiple demonstrations of the same task, since the wrench models of a specific task should not significantly vary between demonstrations. Furthermore, it is purely data-driven and thus there is no assumption regarding the executed task. To the best of our knowledge, the proposed method is the only assessment approach which is able to generalize on a variety of movement reproductions, demonstrations and also it can be applied to different tasks without reprogramming.

## III. MOTION ASSESSMENT PRIMITIVES

We formulate the wrench models as Gaussian Process (GP) which learn a mapping from the pose at each time-step to each dimension of the observed wrench. Then we extract features for a given task by measuring similarities between the GP distributions of a movement reproduction and its corresponding demonstration via the Hellinger distance metric. Consequently, the extracted feature vectors are used to train a Naive Bayes classifier which creates the assessment model. The structure of the proposed method is illustrated in Fig. 2.

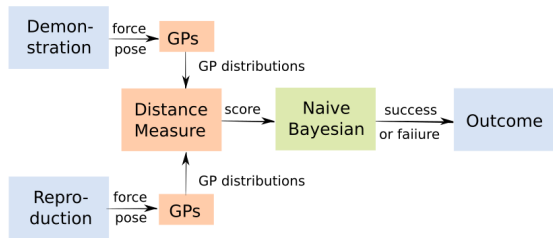


Fig. 2: The overall scheme of the movement assessment primitives. We train Gaussian Processes (GPs) models from a movement demonstration and a set of reproductions. Then their distances are calculated and used as input features for training a probabilistic classifier.

### A. GPs as Wrench Models

Training of MAPs requires data about the pose, time and end-effector wrench during a movement demonstration and its reproductions. For each recorded demonstration with time stamps  $\mathbf{t} \in \mathbb{R}^N$ , we assume that its corresponding reproduction have the same duration with  $N$  number of time-steps. This assumption can be straightforwardly fulfilled by applying data processing methods such as Dynamic Time Warping [16].

The end-effector's pose at each time step is calculated with reference to the final desired pose. This happens to make the method invariant to different starting and goal states. Thus matrices  $\mathbf{X} \in \mathbb{R}^{N \times 3}$  and  $\mathbf{Q} \in \mathbb{R}^{N \times 4}$  represent the relative Cartesian position and orientation w.r.t the target pose at each time-step  $N$  of the movement. The inputs' matrix of the wrench models are represented as:  $\mathbf{D} = [\mathbf{t}, \mathbf{X}, \mathbf{Q}]$

The model's output is the applied wrench, thus the target values consist of the observed wrench signals  $\mathbf{W} \in \mathbb{R}^{N \times 6}$  during the movement. Since a wrench signal is a six dimensional vector each dimension  $w_k$  is modeled separately as:

$$w_k = f_k(\mathbf{D}) + \varepsilon \quad (1)$$

where  $k$  denotes the index of wrench dimensions and  $\varepsilon$  noise of zero mean and  $\sigma^2$  variance.

This mapping is modeled by a Gaussian Process with zero mean and a covariance function:

$$f_k(\mathcal{D}) \sim \mathcal{GP}(\mathbf{0}, \mathbf{K}_k(\mathbf{D})) \quad (2)$$

where  $\mathbf{K}_k(\mathbf{D})$  is the co-variance matrix of each wrench component with elements:

$$\mathbf{K}_k = k_{n,m}(\mathbf{d}_n, \mathbf{d}_m) \quad (3)$$

where  $\mathbf{d}_n$  is the  $n$ th row of data matrix  $\mathbf{D}$  and  $k_{n,m}$  is the  $(n, m)$  element of  $\mathbf{K}$ .

The covariance matrix specifies the properties of the distribution from which the function  $f_k(\mathbf{D})$  is sampled. We use a square-exponential kernel function and a constant noise as follows:

$$k(\mathbf{d}_n, \mathbf{d}_m) = \theta_0 \exp\left(-\frac{\theta_1}{2} (\|\mathbf{t}_n - \mathbf{t}_m\|^2 + \|\mathbf{x}_n - \mathbf{x}_m\|^2 + \phi_e)\right) + \sigma_{m,n}^2$$

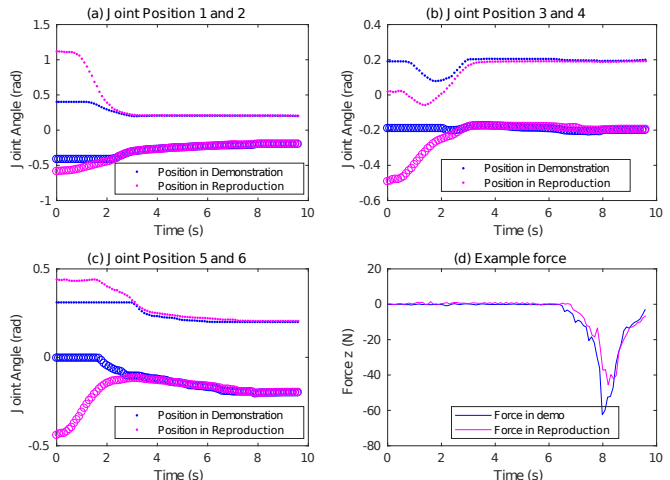


Fig. 3: Example illustrating the properties of GP models. (a-c) 6 pairs of position signals of a demonstration (blue) and corresponding reproduction (magenta) that initially differ greatly before converging. (d) A pair of slightly-different force signals to be modeled by MAPs.

where  $\sigma_{m,n} = 0$ , for  $m \neq n$  specifies the noise variance of the data. The variable  $\phi_e$  is the angular distance between the quaternion components of  $\mathbf{d}_n$  and  $\mathbf{d}_m$ . Hyper-parameters  $\sigma^2$ ,  $\theta_0$  and  $\theta_1$  are components of vector  $\boldsymbol{\theta}$  which are optimized to fit the data by maximizing the log marginal likelihood:

$$\ln p(\mathbf{w}_k | \boldsymbol{\theta}, \mathbf{D}) = -\frac{1}{2} \ln |\mathbf{K}| - \frac{1}{2} \mathbf{w}_k^T \mathbf{K}^{-1} \mathbf{w}_k - \frac{N}{2} \ln(2\pi). \quad (4)$$

where  $\mathbf{w}_k$  is a column vector which contains the observations of the  $k$ th wrench component. As result, we obtain the optimized kernel matrix and thus the GP distribution over the latent function of wrench model (2).

The GP models are invariant to different starting states of a movement. This fact is elaborated schematically in Fig.3 where 6 position profiles of a movement demonstration (magenta) and a reproduction (blue) are illustrated ( Fig.3 (a) (b) (c)). The movements start at different states compared to the demonstration but they quickly converge. Meanwhile, the exerted force profile in Fig.3 (d) is zero at the beginning of the movement and takes values only near the movement's goal state. Thus, GPs model zero wrench at the beginning of movements regardless of their initial state. Furthermore, the use of a zero-mean GP (2) facilitates this generalization. The model assumes *a priori* that states of the movement reproduction which are distant to the demonstrated states do not provide any wrench.

Furthermore, the optimization of the log likelihood (4) depends on the first two terms since the last one is constant. The first penalizes complex models while the second rewards the fit to the training data. Thus, the variation of position signals does not change the second term of the likelihood when the exerted wrench is zero (starting states of the movement). Consequently, the parameters will not be affected during optimization. Furthermore, the influence of various start positions on the first term in (4) is also limited since

this term penalizes the model's complexity. As a result, the model is determined by the force and position signals during the contact between the manipulator and the environment.

### B. Similarity Features

The assessment primitives should be applicable to movement reproductions of any demonstration. Also, a successful movement reproduction should exert similar wrench with the demonstration. Nevertheless, not all the wrench components are significant for assessing a movement. Therefore, a separate similarity measurement is calculated for each wrench component and is used as feature representing the task's characteristics. Thus, the similarity measurements derive based on the previously introduced wrench models of a reproduction and the corresponding demonstration.

Among several options, we compare the GP models between demonstration and movement reproductions with Hellinger distance [17] which is a symmetric measurement of probability distributions' bounded between 0 and 1. Since the GP has analytic integral and we define a zero mean for the model, the Hellinger distance of two GPs is written as:

$$h_k(\mathcal{GP}_k^{\text{demo}}, \mathcal{GP}_k^{\text{rep}}) = \sqrt{1 - \frac{\sqrt[4]{|\mathbf{K}_k^{\text{demo}}| |\mathbf{K}_k^{\text{rep}}|}}{\sqrt{\frac{1}{2} |\mathbf{K}_k^{\text{demo}} + \mathbf{K}_k^{\text{rep}}|}}} \quad (5)$$

where  $\mathcal{GP}_k^{\text{demo}}$  and  $\mathcal{GP}_k^{\text{rep}}$  are the GPs' distributions of  $k^{\text{th}}$  wrench component for the movement's demonstration and reproduction respectively.

However, different demonstrations of the same task may produce various amount of wrench. In order to cope with that, the Hellinger distance of each wrench component is weighted by the total wrench dissimilarity as:

$$m_k = \frac{h_k(\mathcal{GP}_k^{\text{demo}}, \mathcal{GP}_k^{\text{rep}})}{\sum_{k=1}^6 h_k(\mathcal{GP}_k^{\text{demo}}, \mathcal{GP}_k^{\text{rep}})}. \quad (6)$$

Thus, each movement reproduction is represented by a six-dimensional features' vector  $\mathbf{m}$  which describes the rate of dissimilarity for each wrench component. This results to a low dimensional feature vector which represents both the high-dimensional demonstrated and reproduced movements.

### C. Assessment Classifier

A set of labeled similarity features  $\mathbf{m}_l$  are used in order to train the assessment classifier, where the label  $l$  denotes either success or failure. Thus, a Naïve Bayes classifier is trained with both successful and failed examples where each component of the feature vector is modeled by a normal distribution as:

$$p(m_k | c_l) = \mathcal{N}(m_k | \hat{\mu}_{kl}, \hat{\sigma}_{kl}). \quad (7)$$

given its class label  $c_l$ . The parameters  $\hat{\mu}_{kl}$ ,  $\hat{\sigma}_{kl}$  of (7) derive by maximum likelihood of estimation.

Given a new movement descriptor  $\mathbf{m}^*$ , the probability to belong in class  $c_l$  is calculated by :

$$p(c_l | \mathbf{m}^*) \propto p(c_l) \prod_{k=1}^6 p(m_k^* | c_l) \quad (8)$$

where  $p(c_l)$  is the prior probability of the class and the  $p(c_l | \mathbf{m}^*)$  indicates the likelihood of feature  $\mathbf{m}^*$  to belong in class  $c_l$

The movement reproduction cannot be exactly identical to human demonstration due to physical limitations. For example, iiwa robot has an impedance setting in the force mode for safety reasons, which bounds the commanded force. Such physical limitations in the robot will result to a constant similarity among movement reproductions, which does not affect the classifier. Additionally, Naïve Bayes also aggregates the similarities from different wrench dimensions since, according to (8), the distributions of dimensions with less variance have bigger impact on the classification.

The training and application of our method for motion assessment is shown in Algorithm 1.

---

#### Algorithm 1: Motion Assessment Primitives

---

**Train Movement Assessment Primitives;**

**Given :**  $\mathbf{D}^{\text{demo}}, \mathbf{W}^{\text{demo}}$  demonstrated movement data,  
 $\mathbf{D}^{\text{rep}}, \mathbf{W}^{\text{rep}}$  movement reproductions' data,  
 $l$  class labels of reproductions.

**Output:** Naïve Bayes model

- Subtract the movement's goal pose from  $\mathbf{D}^{\text{demo}}$
- Create  $k$   $\mathcal{GP}^{\text{demo}}$  models for each wrench components
- **for** each movement reproduction
  - Subtract the movement's goal pose from  $\mathbf{D}^{\text{rep}}$
  - Create  $k$   $\mathcal{GP}^{\text{rep}}$  models of each wrench component.
  - Obtain similarity features  $m_k$  through Hellinger Distances between  $\mathcal{GP}_k^{\text{rep}}$  and  $\mathcal{GP}_k^{\text{demo}}$

**end**

- Train a Naïve Bayesian classifier given similarity features  $\mathbf{m}$  and class labels  $l$

**Apply Movement Assessment Primitives;**

**Given :**  $\mathbf{D}^{\text{demo}}, \mathbf{W}^{\text{demo}}$  demonstrated movement data,  
 $\mathbf{D}^*, \mathbf{W}^*$  data of movement to be assessed

- Subtract the movement's goal pose from  $\mathbf{D}^{(\text{demo})}$
  - Subtract the desired goal pose from  $\mathbf{D}^*$ ;
  - Create  $k$   $\mathcal{GP}^{\text{demo}}$  models of each wrench component;
  - Create  $k$   $\mathcal{GP}^*$  models of each wrench component;
  - Obtain similarity features  $m_k^*$  through Hellinger Distances between  $\mathcal{GP}_k^*$  and  $\mathcal{GP}_k^{\text{demo}}$ ;
  - Obtain class label  $l$  based on  $\mathbf{m}^*$  via the Naïve Bayes classifier
- 

## IV. EVALUATION

A KUKA iiwa light-weight robot equipped with an ATI F/T sensor is used for trajectory demonstration and reproduction. We obtain the demonstrated pose via kinesthetic teaching, and the corresponding wrench signals from the force/torque sensor mounted at the end-effector. The experiment setup is illustrated in Figure 4. Furthermore, Dynamic Movement Primitives (DMPs) [1] are used to demonstrate movements which are then reproduced with different initial and goal poses, as illustrated in Fig. 4.

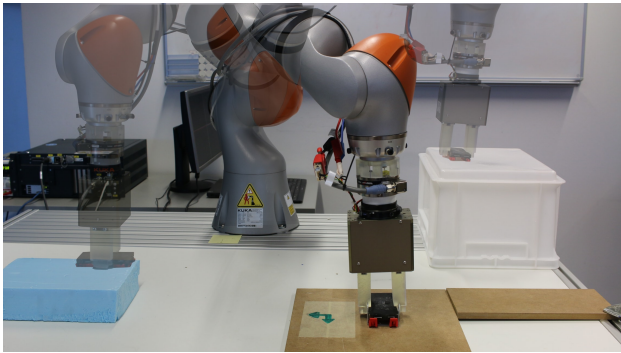


Fig. 4: The experiment setup. The robot executes learned skill for the task with different initial (shadow robot) and goal (solid robot) poses. The data collected are used for training Motion Assessment Primitives (MAPs).

TABLE I: Overview of the datasets

Task	Number of demos	Number of trajectories	Samples per trajectory
Square snap fit	3	60	97
Round snap-fit	3	60	143
Screwing	3	60	204
Twitter snap-fit	1	15	79
Speaker Screwing	1	15	178

The proposed method is evaluated on snap-fit assembly and screwing which are common force-interaction tasks in manufacturing. Therefore, we design three toy-cases and also use two industrial use-cases of snap-fitting and screwing. The toy-cases include square snap-fit assembly (Fig. 5), round snap-fit assembly (Fig. 6) and screwing (Fig. 7). The industrial use cases are subtasks of a vehicle’s audio-system assembly provided by Magna Steyr. It consists of a tweeter insertion with snap-fit and speaker screwing which are challenging to perform without force control.

For each toy-case, we collect 3 datasets associated with 3 different demonstrations. Each dataset consists of time-stamps, wrench signals, Cartesian poses and labels regarding the outcome of 20 task executions which are used to train the Naive Bayes classifier. TABLE I provides an overview of all the gathered datasets.

The proposed method’s generalization ability is evaluated on two scenarios: the states’ variation and demonstrations’ variation. In the first case, the classifier is trained from a set of movements’ generated by DMPs from a specific demonstration. Then the classifier assesses the outcome of movement generated by the same DMP but with different starting and target states. In the more challenging scenario of demonstrations’ variation, the classifier assesses movements which are generated by different demonstrations.

#### A. Toy-cases

We design three toy use-cases of varying complexities. For each of those, three demonstrations are performed from

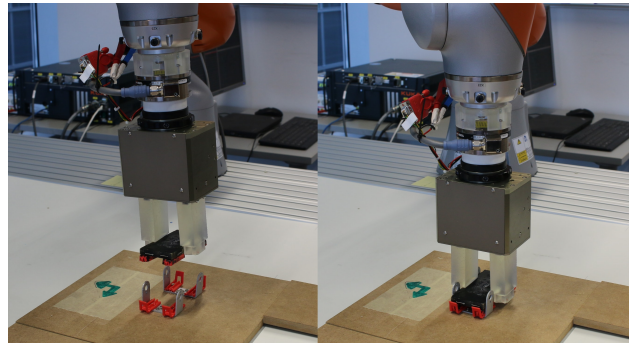


Fig. 5: Square snap-fit assembly toy-case. The robot inserts the manipulated object into the base with 4 snap-fits (red). The motion is constrained by 4 metal parts (grey) on the base (left). All four snap-fits have to be inserted (right).

different individuals which create three data sets to verify the generalization capabilities of MAPs. For each demonstration, we first let the robot execute DMPs 10 times with random initial and goal positions that vary on a large scale. We then perform 10 movement reproductions which result in failure due to inaccurate goal positions or pose variations of the work-pieces.

The first toy use-case is the square snap-fit assembly. As shown in Fig. 5, this setup has 4 ‘L’ shaped cantilever snaps (red). On the base, there are 4 metal parts (grey) that constrain the snap-in movement. Thus, this setup only allows up to 3 mm deviation from demonstrated positions during snapping. The snap-fits can only be inserted in the vertical direction with a fixed pose. The manipulated object (black) to be inserted has notches on its back. If the movement deviates from the demonstration when snapping, the manipulated object will be jammed on the metal parts. When all 4 snap-fits are fully inserted, the execution is successful.

The proposed method’s generalization ability to various start/target states and demonstrations for the square snap-fit is included in first two rows of TABLE II. The movement’s generalization to different start/goal states renders very good performance since dataset 1 and 2 are assessed with more than 90% of accuracy. As for the generalization to different demonstrations, dataset 1 and 2 have good performance with accuracy of more than 75%. It should be noted that 100% of success rate is achieved at dataset 3.

The second use case is a round snap-fit assembly illustrated in Fig. 6. There are 3 ‘L’ shaped cantilever snaps (green)

TABLE II: Assessment accuracy on all the toy-cases

Toy-case:	Generalization to:	Dataset 1	Dataset 2	Dataset 3
Square Snap-fit	Start & Target States	90%	80%	95%
	Demonstrations	75%	75%	100%
Round Snap-fit	Start & Target States	80%	85%	75%
	Demonstrations	75%	75%	70%
Screwing	Start & Target States	80%	75%	75%
	Demonstrations	85%	75%	85%

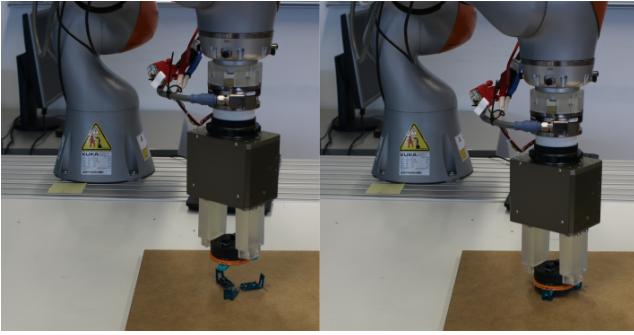


Fig. 6: The round snap-fit assembly toy-case. The robot inserts the manipulated object (black) into the base with 3 snap-fits (green). There is no constraints for the motion (left). The task is completed when all 3 snap-fits are inserted (right).

mounted on a round configuration where there is no physical constraint. A challenge of this task is that there are different ways of demonstration. In our first demonstration, the user firstly inserts one snap and then insert the rest. Likewise, two snaps are inserted at first in our second demonstration. Alternatively, all three snaps are inserted simultaneously in our third demonstration. An execution is classified as a success when all snap-fits are inserted.

The proposed method’s performance at the case of round snap-fit is illustrated in the middle two rows of TABLE II. The start/goal state generalization is more than 80% for the demonstrations 1 and 2 while it is slightly worse for the third one. Furthermore, the generalization to different demonstrations is slightly worse compared to the other tasks. This is due to the large variety of demonstrated assembly policies.

The third toy-case is screwing as shown in Fig. 7 where a M3.5 bolt is fastened on a 3D printed base (black). The bolt appends on the tip of the screw-driver by magnetic force. In order to activate the screw driver, one must rotate clock-wise and simultaneously apply a vertical force. The bolt needs to be fully fastened for successful execution.

Screwing is more complex than square snap-fit assembly,

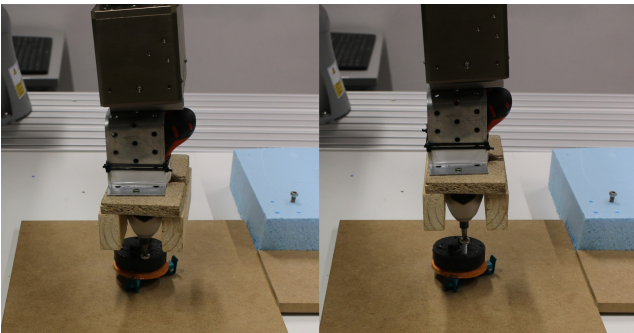


Fig. 7: The screwing toy-case. The robot picks up a M3.5 screw and screws it at the black base (left). The Motion Assessment Primitives (MAPs) verify if the screw is tightened in the hole (right).



Fig. 8: The industrial use cases of vehicle audio assembly. A speaker is mounted on a base with 3 screws (left). A tweeter is inserted in the base with snap-fits (right).

since there is no tight physical constraint for the movement. Even though the task can only be successfully completed in a certain manner, scenarios diverse for failed executions. The tip of the screw will have various behaviors if the screw is not inserted in the hole while screwing. For instance, the screw may rotate on a flat surface, or the screw may be detached from the tip. Thus failed executions do not have similar force profiles which makes this task significantly challenging. Furthermore, since the screw is attached to the tip by magnetic field, the pose of the screw is not exactly identical among different movements. The generalization performance in the screwing toy-case is included in the last two rows of Table II.

In this challenging task, the generalization to different movement states is dropped by about 10% ranging from 75% to 80% compared to the square snap-fit. Similarly, the generalization to different demonstrations is also reduced.

### B. Industrial use-cases

The datasets gathered for toy-cases are created in order to capture a large variety of possible failures. Nevertheless, not all of those failures take place during normal operating conditions. Therefore, MAPs are also evaluated on two industrial use-cases where the robotic system operates as it would within a manufacturing scenario. The industrial use-cases include screwing and snap-fitting which are common force-interaction tasks in industry. As shown in Fig. 8, we need to insert a tweeter with 3 cantilever snap-fits into the base which has physical constraints (right). Concerning screwing, we need to fasten the large speaker on the base with three bolts (right).

Similar to toy-cases, we perform a demonstration for each task and reproduce it with various start and goal positions. Thus, we perform 15 task executions in order to measure the prediction accuracy of the MAP on different executed trajectories. The results of the leave-one-out cross-validation are illustrated in Table III where the algorithm’s accuracy is significantly increased compared to the toy-cases for both screwing and snap-fittings. This happens because failures during normal operation are much less diverse compared to

TABLE III: Assessment accuracy on the industrial use cases

Industrial use-case	Success rate
Screwing	80%
Snap-fitting	93.33%

the failures in the toy-cases datasets.

Furthermore, from the confusion matrices of the industrial use-cases (Table IV) is observed that, in the case of screwing task, the predictions are not biased towards a specific class. Nevertheless, this is not the case for snap-fitting due to its unbalanced dataset which contains two failures. However, this result demonstrates the proposed method’s data-efficiency since it is able to correctly assess a failure even with a single training instance for a class.

TABLE IV: Confusion Matrices for Industrial Use Cases

Screwing			Snap-fitting		
$n = 15$	Predicted: Success	Predicted: Failure	$n = 15$	Predicted: Success	Predicted: Failure
Actual: Success	5	2	Actual: Success	13	0
Actual: Failure	1	8	Actual: Failure	1	1

## V. CONCLUSIONS

In this paper we proposed a novel adaptable, reusable and task-agnostic movement assessment primitive which can be used alongside DMPs in order to form flexible reusable robotic-skills. MAPs assess the reproduced task outcome through a Programming by Demonstration (PbD) method similarly to DMPs. The algorithm consists of two learning models, the first compares the similarity between a movement demonstration and reproduction by calculating the statistical distance of their corresponding wrench models which are represented by GPs. The similarity measurements are fed to the second model – a Naive Bayes classifier – which assigns the probability of success.

The proposed method has been evaluated on five different use-cases of two diverse force-interaction tasks: screwing and snap-fitting. Furthermore, the generalization ability to various demonstrations and movement reproductions has been assessed on a total of 11 demonstrations and 210 trajectories. The experimental results demonstrate an overall good ability of the method to assess motions which are generated either from the same or different demonstrations. Nevertheless, the generalization to various demonstrations appears to be more challenging. Also, the method has to be retrained but not reprogrammed for different tasks (screwing, snap-fitting). This fact significantly increases the re-usability of the proposed primitive which can make it valuable part of skill-based systems. Furthermore, MAPs can be used within reinforcement learning algorithms in order to provide a fast estimate for the quality of the performed movement [18].

Thus, future work can be focused on including such movement assessment methods as evaluation primitives in skill-based systems. Furthermore, the presented method can be expanded with online learning in order to make it capable to assess a predicted motion on-the-fly and also be used as part of a reward function in reinforcement learning.

## REFERENCES

- [1] A. J. Ijspeert, J. Nakanishi, H. Hoffmann, P. Pastor, and S. Schaal, “Dynamical movement primitives: learning attractor models for motor behaviors,” *Neural computation*, vol. 25, no. 2, pp. 328–373, 2013.
- [2] A. Billard, S. Calinon, R. Dillmann, and S. Schaal, “Robot programming by demonstration,” in *Springer handbook of robotics*, pp. 1371–1394, Springer, 2008.
- [3] U. Zimmermann, “Industrial robot and method for programming an industrial robot,” Feb. 2 2016. US Patent 9,250,624.
- [4] A. Billard, S. Calinon, and R. Dillmann, “Learning from humans,” in *Springer handbook of robotics*, pp. 1995–2010, Springer, 2016.
- [5] F. Rovida, M. Crosby, D. Holz, A. S. Polydoros, B. Großmann, R. P. Petrick, and V. Krüger, “SkiROSa skill-based robot control platform on top of ROS,” in *Robot Operating System (ROS)*, pp. 121–160, Springer, 2017.
- [6] L. Xie, J. Zeng, U. Kruger, X. Wang, and J. Geluk, “Fault detection in dynamic systems using the kullback–leibler divergence,” *Control Engineering Practice*, vol. 43, pp. 39–48, 2015.
- [7] A. Montebelli, F. Steinmetz, and V. Kyriki, “On handing down our tools to robots: Single-phase kinesthetic teaching for dynamic in-contact tasks,” in *Robotics and Automation (ICRA), 2015 IEEE International Conference on*, pp. 5628–5634, IEEE, 2015.
- [8] B. S. J. Costa, C. G. Bezerra, L. A. Guedes, and P. P. Angelov, “Online fault detection based on typicality and eccentricity data analytics,” in *Neural Networks (IJCNN), 2015 International Joint Conference on*, pp. 1–6, IEEE, 2015.
- [9] A. Haidu, D. Kohlsdorf, and M. Beetz, “Learning action failure models from interactive physics-based simulations,” in *Intelligent Robots and Systems (IROS), 2015 IEEE/RSJ International Conference on*, pp. 5370–5375, IEEE, 2015.
- [10] J. Rojas, K. Harada, H. Onda, N. Yamanobe, E. Yoshida, K. Nagata, and Y. Kawai, “Towards snap sensing,” *International Journal of Mechatronics and Automation*, vol. 3, no. 2, pp. 69–93, 2013.
- [11] A. Haidu, D. Kohlsdorf, and M. Beetz, “Learning task outcome prediction for robot control from interactive environments,” in *Intelligent Robots and Systems (IROS 2014), 2014 IEEE/RSJ International Conference on*, pp. 4389–4395, IEEE, 2014.
- [12] E. Di Lello, M. Klotzbucher, T. De Laet, and H. Bruyninckx, “Bayesian time-series models for continuous fault detection and recognition in industrial robotic tasks,” in *Intelligent Robots and Systems (IROS), 2013 IEEE/RSJ International Conference on*, pp. 5827–5833, IEEE, 2013.
- [13] A. Fod, M. J. Matarić, and O. C. Jenkins, “Automated derivation of primitives for movement classification,” *Autonomous robots*, vol. 12, no. 1, pp. 39–54, 2002.
- [14] S. Calinon, F. Guenter, and A. Billard, “On learning, representing, and generalizing a task in a humanoid robot,” *IEEE Transactions on Systems, Man, and Cybernetics, Part B (Cybernetics)*, vol. 37, no. 2, pp. 286–298, 2007.
- [15] P. Pastor, M. Kalakrishnan, S. Chitta, E. Theodorou, and S. Schaal, “Skill learning and task outcome prediction for manipulation,” *2011 IEEE International Conference on Robotics and Automation*, pp. 3828–3834, 2011.
- [16] M. Gienger, M. Mühligh, and J. J. Steil, “Imitating object movement skills with robots a task-level approach exploiting generalization and invariance,” in *Intelligent Robots and Systems (IROS), 2010 IEEE/RSJ International Conference on*, pp. 1262–1269, IEEE, 2010.
- [17] R. Lourenzutti and R. A. Krohling, “The hellinger distance in multicriteria decision making: An illustration to the topsis and todim methods,” *Expert Systems with Applications*, vol. 41, no. 9, pp. 4414–4421, 2014.
- [18] A. S. Polydoros and L. Nalpantidis, “Survey of model-based reinforcement learning: Applications on robotics,” *Journal of Intelligent & Robotic Systems*, vol. 86, pp. 153–173, May 2017.